Simultaneous optical model analysis of elastic scattering, fusion, and breakup for the ^{9}Be + ^{144}Sm system at near-barrier energies

A. Gómez Camacho*
Departamento del Acelerador, Instituto Nacional de Investigaciones Nucleares, Apartado Postal 18-1027, C. P. 11801, México D. F. Centro, México

P. R. S. Gomes and J. Lubian
Instituto de Fisica, Universidade Federal Fluminenese, Avenida Litoranea s/n, Gragoatá, Niterói, RJ 24210-340, Brazil

I. Padrón
Centro de Aplicaciones Tecnológicas y Desarrollo Nuclear, Playa, Ciudad de la Habana, Cuba
(Received 8 February 2008; revised manuscript received 27 March 2008; published 23 May 2008)

A simultaneous optical model calculation of elastic scattering, complete fusion, and breakup cross sections for energies around the Coulomb barrier is presented for reactions involving the weakly bound projectile ^{9}Be on the medium size target ^{144}Sm. In the calculations, the nuclear polarization potential U is split into a volume part U_F, which is responsible for fusion reactions, and a surface part $U_{\rm DR}$, which accounts for direct reactions. A simultaneous χ^2 analysis of elastic and complete fusion data shows that the extracted optical potential parameters of the real V_F and imaginary W_F parts of U_F and the corresponding parts $V_{\rm DR}$ and $W_{\rm DR}$ of $U_{\rm DR}$ satisfy separately the dispersion relation. Energy-dependent forms for the fusion and direct reaction potentials indicate that, at the strong absorption radius, the direct reaction potentials dominate over the fusion potentials. Moreover, the imaginary direct reaction potential results in a rather smooth function of E around the barrier energy. These findings show that the threshold anomaly, usually present in reactions with tightly bound projectiles, is not exhibited for the system ^{9}Be + ^{144}Sm. Within this formalism, the effect of breakup reactions on complete fusion is studied by turning on and off the potentials responsible for breakup reactions.

DOI: 10.1103/PhysRevC.77.054606 PACS number(s): 25.70.Jj, 24.10.Ht, 25.60.Gc, 25.70.Mn

I. INTRODUCTION

Lately, special interest has been focused on the role that the breakup process plays on fusion and other reaction mechanisms in reactions involving weakly bound nuclei. Similarly, intense research has been done concerning the presence of the threshold anomaly in the elastic scattering of those nuclei. The most studied systems with weakly bound projectiles are those that include ^{9}Be,^{6} Li,^{7} Li, and ^{6}He. The breakup separation energies for these nuclei are relatively small, for instance, $^{9}\mathrm{Be} \Longrightarrow {}^{8}\mathrm{Be} + n \Longrightarrow \alpha + \alpha + n$ with $S_n = 1.67$ MeV or $^{9}\mathrm{Be} \Longrightarrow {}^{5}\mathrm{He} + \alpha$ with $S_\alpha = 2.55$ MeV, $^{6}\mathrm{Li} \Longrightarrow \alpha + d$ with $S_\alpha = 1.48$ MeV, $^{7}\mathrm{Li} \Longrightarrow \alpha + t$ with $S_\alpha = 2.47$ MeV, and $^{6}\mathrm{He} \Longrightarrow {}^{4}\mathrm{He} + 2n$ with $S_{2n} = 0.98$ MeV. Owing to the small breakup separation energies, reactions with these projectiles show a strong breakup coupling, particularly below the barrier energy, that has an important effect on fusion and other reaction processes. However, reactions with these weakly bound projectiles with a variety of targets with masses ranging from medium to heavy show that the breakup yield has considerable values even for energies well below the Coulomb barrier. Therefore, it is a point of discussion that the threshold anomaly (TA) usually observed in the scattering of tightly bound nuclei should not be present in the scattering of weakly bound projectiles. It is well known that the TA is related to a strong variation of the optical potential around the Coulomb barrier. That is, the energy dependence of the strength of the imaginary part of the optical potential shows a sharp decrease as the bombarding energy approaches the barrier energy V_B. The corresponding strength for the real part of the optical potential also varies very strongly around the barrier [1,2]. It has recently been proposed that reactions involving the most weakly bound nuclei show a different type of anomaly, the so-called breakup threshold anomaly (BTA) [3–5], in which, in contrast to the TA, the absorptive part of the nuclear potential $W(E)$ does not show a strong decrease as the bombarding energy approaches the Coulomb barrier energy. Actually, $W(E)$ increases even below the barrier V_B. Consequently, the energy dependence of the real part of the optical potential $V(E)$, derived from $W(E)$ by the dispersion relation, does not show the usual bell-shape around V_B associated with the TA.

With the purpose to investigate the presence of the TA or other forms of behavior of the optical potential, several studies have been done on reactions with stable weakly bound projectiles on heavy and medium mass targets. The studies of Keeley and co-workers [6,7] for ^{6}Li and ^{7}Li incident on ^{208}Pb show that for $^{7}\mathrm{Li} + {}^{208}\mathrm{Pb}$ the usual TA shows up, which is not the case for $^{6}\mathrm{Li} + {}^{208}\mathrm{Pb}$. Accordingly, this fact is linked to the experimental result that the system $^{6}\mathrm{Li} + {}^{208}\mathrm{Pb}$ shows a higher α-breakup yield below the barrier energy than $^{7}\mathrm{Li} + {}^{208}\mathrm{Pb}$. Since ^{9}Be has a breakup threshold energy close to that for ^{6}Li, these authors suggest that the threshold anomaly should also be absent for reactions involving ^{9}Be. However, Woolliscroft *et al.* [8,9] show that for the system $^{9}\mathrm{Be} + {}^{208}\mathrm{Pb}$, despite the high breakup and $1n$-transfer cross

*Corresponding author: agc@nuclear.inin.mx

section yields at sub-barrier energies, the usual TA is still present. In another work for a similar system, ^{9}Be + ^{209}Bi, Signorini and co-workers [10–12] do not come to any definitive conclusion about the threshold anomaly, owing to the small number of data below the Coulomb barrier.

South American groups [13–26] and a European collaboration led by Pakou [27–30] have extensively studied reactions of stable weakly bound beams of ^{6}Li, ^{7}Li, and ^{9}Be on light mass targets such as ^{27}Al, ^{28}Si, and ^{64}Zn. From these studies, it has been determined that the usual TA is not present for reactions involving the projectiles ^{6}Li and ^{9}Be. For the case of medium mass targets, the only systems studied so far are ^{6,7}Li + ^{138}Ba [5,31], and the results are basically the same as those found by Keeley and co-workers [6,7] for ^{6,7}Li + ^{208}Pb. The main explanation for these results is that the appreciable cross section observed for the ^{6}Li breakup channel at low energies, which in fact accounts for most of the total reaction cross section, does not allow the decrease of the imaginary absorptive potential. For ^{7}Li-induced reactions, the breakup cross section yield is not large, possibly because of its higher α-breakup energy ($S_\alpha = 2.47$ MeV), and different conclusions are found. For scattering of the halo radioactive ^{6}He nucleus, the uncertainties and paucity of data did not allow definitive conclusions to be drawn about the presence of the TA [32–35]. Very recently, some evidence has come to light for the presence of BTA in the scattering of ^{6}He by heavy targets [36,37]. For the ^{9}Be projectile, the behavior of elastic scattering is not yet fully understood. In fact, different authors find conflicting results about the TA for reactions of ^{9}Be with several targets such as ^{208}Pb [8,9], ^{209}Bi [10–12], and ^{64}Zn [16,17,38].

The different results found in the study of the TA for systems involving weakly bound nuclei should be related not only to the value of the breakup threshold energy of the projectile but also to the characteristics of the target. This is because the breakup has contributions from the nuclear and Coulomb breakups. Whereas the first is dominated by projectile structure details, Coulomb breakup is more concerned with the dynamics of the reaction and the target. For weakly bound projectiles and heavy targets, the Coulomb breakup is very strong and its effects on the surface optical potential are different from that of the nuclear breakup [39–41]. Therefore, it is a very interesting subject of research to continue the investigation of reactions of ^{9}Be on other targets, especially on medium mass targets such as ^{144}Sm, a target mass region not yet studied with this projectile, and so to contribute to elucidate the source of the discrepancies about the TA.

In this work, we consider the extensive measurements for the reaction between ^{9}Be with the medium mass target ^{144}Sm [18,42] and perform a theoretical study of them using the optical model for direct reactions. A preliminary short version of these calculations has been published as a proceedings contribution [43]. In this work we perform a simultaneous calculation of elastic scattering, complete fusion, and breakup cross sections within the optical model. Particular emphasis focuses on two aspects: the TA and the effect that the breakup process has on fusion.

We consider, in the following analysis, that both the real and imaginary parts of the optical potential contain a volume and a surface part, since different reactions occur at different distances and therefore give rise to potentials of different forms. This concept has been widely used in the literature [44–49]. Satchler and collaborators [50–54] consider that, at near-barrier energies, the volume part of the potential corresponds to the absorption into fusion and has a short range, corresponding to a reduced radius r_F of the order of 1.0 fm and diffuseness of the order of 0.25 fm. For these values, these authors successfully obtained simultaneous fits of fusion and elastic scattering within a coupled channel calculations approach, which takes into account coupling to direct reaction channels. Udagawa and collaborators and other authors [55–60] were also very successful in fitting simultaneously near-barrier fusion and elastic scattering data using an alternative approach. These authors also propose dividing the total imaginary potential W into an inner potential responsible for fusion W_F and a surface potential $W_{\rm DR}$, but in this approach, $W_F = W$ for $r < R_F$ and $W_F = 0$ for $r > R_F$, where $R_F = r_F(A_1^{1/3} + A_2^{1/3})$ and r_F is treated as an adjustable parameter to fit simultaneously fusion and elastic scattering data. From this approach, it is assumed that the volume part, W_F, is solely responsible for the complete fusion absorption process whereas the surface part, $W_{\rm DR}$, is responsible for all other absorption processes. For several systems, these authors found values of r_F around 1.4 fm, corresponding to a long=range fusion potential. In the present work, the approach used is the one proposed by Udagawa and co-workers [55,61] to describe fusion within the framework of direct reaction theory. Thus, a Woods-Saxon optical potential $U_a = V_a + iW_a$ for the entrance channel a is considered, where the imaginary potential W_a is split into volume and surface parts; that is, $W_a = W_{a,F} + W_{a,\rm DR}$.

We propose that by means of the decomposition of W_a, the effect of the breakup of the projectile on fusion will be more clearly isolated. It is expected that the conjugated energy dependence of the fusion potential $W_{a,F}$ and the direct reaction potential $W_{a,\rm DR}$ will tell us the strength of the breakup effect on fusion. For the system ^{9}Be + ^{144}Sm, direct reactions are mostly breakup reactions, particularly near and below the Coulomb barrier; hence they should be treated by $W_{a,\rm DR}$. Actually, it has been reported [18,42] that the inelastic excitations of the ^{144}Sm target have cross sections of the order of 10% of breakup reactions for energies in the range from $0.9V_B$ to V_B, where V_B is the barrier energy. However, for these low energies there are no available complete elastic angular distributions that could be studied in the present work. For the energy range studied here ($31 < E_{\rm c.m.} < 39$ MeV), inelastic cross sections were found to be less than 5% of the total reaction cross section [18,42].

The Woods-Saxon parameters of the optical potentials will be extracted by a simultaneous χ^2 analysis of complete fusion and elastic scattering data. The direct reaction cross section $\sigma_{\rm DR} = \sigma_R - \sigma_{\rm CF}$ includes incomplete fusion $\sigma_{\rm ICF}$, inelastic scattering $\sigma_{\rm inel}$, and noncapture breakup $\sigma_{\rm NCBU}$. In fact, $\sigma_{\rm NCBU}$ for the nuclear system under consideration accounts for most of the total reaction cross section at energies below the Coulomb barrier.

The TA is studied by considering the energy-dependent potentials $V_{a,F}(E)$, $V_{a,\rm DR}(E)$, $W_{a,F}(E)$, and $W_{a,\rm DR}(E)$ at the strong absorption radius $R_{\rm sa}$. Here, $V_{a,F}(E)$ and $V_{a,\rm DR}(E)$ are

the real parts of the fusion and direct reaction potentials and the strong absorption radius R_{sa} is defined as the distance at which the elastic S matrix takes the value $|S_{el}(R_{sa})|^2 = 1/2$. The effect of breakup reactions on complete fusion is analyzed by studying the effects of $V_{a,DR}(E)$ and $W_{a,DR}(E)$ on the fusion cross-section calculation.

The paper is organized as follows: In Sec. II a brief description of the model is presented. In Sec. III, the χ^2 analysis of the data and the results of the calculations are given. The paper is concluded with Sec. IV, which is dedicated to a brief summary and conclusions.

II. METHODOLOGY USED

The Hamiltonian H for the nuclear system is of the form

$$H_a = T_a + \mathcal{V}_a, \tag{1}$$

where the distorted wave $\chi_a^{(+)}$satisfies the following expression:

$$(T_a + \mathcal{V}_a)\chi_a^{(+)} = E_a\chi_a^{(+)}, \tag{2}$$

and the potential $\mathcal{V}_a$ is defined by

$$\mathcal{V}_a(r, E) = V_{Coul}(r) - V_{a,0}(r) - U_a(r, E). \tag{3}$$

Here, $V_{Coul}(r)$ is the Coulomb potential, $V_{a,0}(r)$ is the energy-independent average nucleus-nucleus potential as defined in Ref. [62], and $U_a(r, E)$ is the nuclear polarization potential, which is given by [63–65]

$$U_a(r, E) = V_a(r, E) + iW_a(r, E). \tag{4}$$

To simplify the notation, we will drop the subindex a, which refers to the incident elastic channel. Then, the imaginary part W is assumed to have two parts, that is,

$$W(r, E) = W_F(r, E) + W_{DR}(r, E), \tag{5}$$

where W_F accounts for complete fusion and W_{DR} for all other absorption processes. Thus, Eq. (4) can be written as $U = U_F + U_{DR}$, where $U_F = V_F + iW_F$ and $U_{DR} = V_{DR} + iW_{DR}$ with $V = V_F + V_{DR}$.

The strength of the real polarization potentials V_F and V_{DR} can be derived from the imaginary potential strengths $W_F(E)$ and $W_{DR}(E)$ by the dispersion relation

$$V_i(E) = V_i(E_s) + \frac{(E - E_s)}{\pi}\mathcal{P}\int_0^\infty \frac{W_i(E')}{(E' - E_s)(E' - E)}dE', \quad i = F, \text{DR}, \tag{6}$$

where $V_i(E_s)$ is the value of the potential at the reference energy E_s as defined in Ref. [2]. So, once the energy-dependent forms for $W_i(E)$, $i = F$, DR are calculated, the corresponding real potentials $V_i(E)$ can be found. It should be pointed out that these energy-dependent forms for the strengths $W_i(E)$, $i = F$, DR, in the range from zero to infinity are determined by fitting (normally by linear segments) the adjusted values found by the χ^2 analysis of the experimental data [1,2].

The energy-independent average nuclear potential $V_0(r)$ and the fusion absorption potential $W_F(r, E)$ are assumed to have the geometrical forms

$$V_0(r) = V_0 f(r) \tag{7}$$

and

$$W_F(r, E) = W_F(E) f(r), \tag{8}$$

where

$$f(x_i) = \frac{1}{1 + \exp(x_i)}, \quad x_i = \frac{r - R_i}{a_i}, \quad i = 0, F. \tag{9}$$

with $R_i = r_i(A_1^{1/3} + A_2^{1/3})$, r_i being the reduced radius parameter and a_i the diffuseness parameter.

The surface imaginary potential $W_{DR}(r, E)$ is defined by

$$W_{DR}(r, E) = 4a_{DR}W_{DR}(E)\frac{df(x_{DR})}{dr}, \tag{10}$$

where a_{DR} stands for the direct reaction diffuseness and $x_{DR} = (r - R_{DR})/a_{DR}$. The potentials $V_F(r, E)$ and $V_{DR}(r, E)$ are assumed to have the same forms as $W_F(r, E)$ and $W_{DR}(r, E)$, respectively, with the same diffuseness and reduced radius. The parameters of $V_0(r)$, $W_F(r, E)$, and $W_{DR}(r, E)$ as well as the strengths of $V_F(r, E)$ and $V_{DR}(r, E)$ will be extracted from a simultaneous χ^2 analysis of the elastic and complete fusion data, as will be shown in the next section. It should be pointed out that the breakup cross section may include contributions from Coulomb and nuclear interactions, and therefore the direct reaction potential may include both effects. Also, the average nucleus-nucleus potential $V_0(r)$ of Eq. (3) may have an energy dependence from nonlocality effects coming from a knockon-exchange contribution. We shall not consider such effects since they are negligible [51].

The radial-angle-integrated total reaction cross section is calculated by using the full absorption potential W, that is,

$$\sigma_R(E) = \frac{2}{\hbar v}\langle\chi_a^{(+)}|W(E)|\chi_a^{(+)}\rangle, \tag{11}$$

where we have rewritten the subindex a to emphasize the elastic channel. The fusion and direct reaction cross sections are similarly obtained by

$$\sigma_i(E) = \frac{2}{\hbar v}\langle\chi_a^{(+)}|W_i(E)|\chi_a^{(+)}\rangle, \quad i = F, \text{DR}. \tag{12}$$

The relative motion distorted waves $\chi_a^{(+)}$ are solutions of Eq. (2) with the full Woods-Saxon potential U_a of Eq. (4). These will be used throughout the calculations; therefore all the calculated cross sections will be consistent with elastic scattering.

The fusion cross section $\sigma_F(E)$ as given by Eq. (12) has been used in a number of studies by Udagawa and collaborators in reactions with stable tightly bound nuclei [55,61,66,67], as well as with weakly bound ones [59,68,69].

III. DESCRIPTION OF THE CALCULATIONS AND RESULTS

A. Simultaneous χ^2 analysis of elastic scattering and complete fusion

We start this section by presenting the definitions of complete fusion and other mechanisms associated with breakup

and total fusion [70]. Complete fusion (CF) is the fusion of the whole projectile with the target. In addition to the sequential complete fusion (SCF) process, the breakup of the projectile (BU) is a direct reaction process that can lead to two other different reaction mechanisms: 1. noncapture breakup (NCBU), which occurs when neither of the fragments is captured by the target, and 2. incomplete fusion (ICF), which is the fusion of part of the projectile with the target that follows the breakup of the projectile. These mechanisms depend on the subsequent interactions between the projectile fragments and target nucleus. The total breakup cross section is given by $\sigma_{\rm BU} = \sigma_{\rm NCBU} + \sigma_{\rm ICF}$. Total fusion (TF) is the sum of CF with all possibilities of ICF.

As for the ^{9}Be projectile, fusion of ^{8}Be with the target following $^9\mathrm{Be} \Longrightarrow {}^8\mathrm{Be} + n$ is considered as a CF mechanism. This is so since it is not possible to experimentally distinguish this process from the fusion of ^{9}Be with the target [42,71, 72]. Thus, what one calls ICF for the $^9\mathrm{Be} + {}^{144}\mathrm{Sm}$ system is the fusion of one α particle with the target, following the sequential breakup $^9\mathrm{Be} \Longrightarrow {}^8\mathrm{Be} + n \Longrightarrow \alpha + \alpha + n$. For the reaction $^9\mathrm{Be} + {}^{144}\mathrm{Sm}$, $\sigma_{\rm ICF}$ was found experimentally to be of the order of 10% of $\sigma_{\rm TF}$ at low energies [18,42]. The total reaction cross section is thus $\sigma_R = \sigma_{\rm BU} + \sigma_{\rm CF} + \sigma_{\rm inel}$, where the breakup cross section $\sigma_{\rm BU}$ is the sum of the noncapture breakup cross section $\sigma_{\rm NCBU}$ and that of incomplete fusion, $\sigma_{\rm ICF}$. An estimation of the inelastic cross section $\sigma_{\rm inel}$ has been given in Refs. [18,42] for the excitation of the first $2^+$and 3^- states of the target. In this work, a calculation of σ_R-$\sigma_{\rm CF}$ will be compared to the experimental values of $\sigma_{\rm NCBU} + \sigma_{\rm ICF} + \sigma_{\rm inel}$.

Now, we begin the calculations by performing a simultaneous χ^2 analysis of elastic scattering and CF data for the system $^9\mathrm{Be} + {}^{144}\mathrm{Sm}$ at the energies $E_{\rm lab} = 33, 34, 35, 37, 39,$ and 41 MeV. As a first step, we search the potential V_0 of Eqs. (3) and (7), which is an energy-independent potential related to the relative motion of the interacting nuclei [62]. The parameters of this average potential $V_0(r)$ can be found by fitting the elastic scattering data at the energy $E_{\rm lab} = 32$ MeV. Since this potential is energy independent this can be determined at any chosen energy. As an absorption potential, we choose a volume Woods-Saxon potential with parameters $r_W = 1.4$ fm, $W = 64.3$ MeV, and $a_W = 0.36$ fm. As mentioned before, $r_F = 1.4$ fm is a value found for simultaneous fits of fusion and elastic scattering data for a large variety of systems [55–60]. The derived parameters for $V_0(r)$ are $V_0 = 25$ MeV, $r_0 = 1.22$ fm, and $a_0 = 0.52$ fm, which correspond to a shallow potential, similar to the ones required in the fit of elastic scattering data of weakly bound projectiles such as ^{6}Li and ^{9}Be [51]. This derived real potential predicts the height and position of the Coulomb barrier as 32 MeV and 10.2 fm, respectively, for the angular momentum $l = 0$.

Now, to fit the elastic scattering angular distributions and fusion cross sections, we use the following parametrization for the fusion potential $W_F(r, E)$. The radius parameter r_F is fixed at 1.4 fm and thus the strength $W_F(E)$ and the diffuseness a_F are calculated by the χ^2 analysis. For the surface potential $W_{\rm DR}(r, E)$, we set $a_{\rm DR} = 0.72$ fm, then $W_{\rm DR}(E)$ and the reduced radius $r_{\rm DR}$ are calculated. Since the geometric forms of $V_F(r, E)$ and $V_{\rm DR}(r, E)$ are assumed to be the same as $W_F(r, E)$ and $W_{\rm DR}(r, E)$, respectively, with the same reduced radius and diffuseness parameters, only the energy-dependent strengths $V_F(E)$ and $V_{\rm DR}(E)$ are also determined in the χ^2 analysis. So, in Figs. 1(a) and 1(b), we show the results for the potential strengths $W_F(E)$, $W_{\rm DR}(E)$, $V_F(E)$, and $V_{\rm DR}(E)$, which are represented by the dots; in Table I, the calculated values for a_F and $r_{\rm DR}$ are presented. For the energy range investigated, near the Coulomb barrier, one can observe fluctuations in the value of the diffuseness a_F, compatible with an energy-dependent behavior of W_F, typical of near-barrier energy scattering.

TABLE I. Calculated values for the diffuseness $a_F$and reduced radius $r_{\rm DR}$ of the fusion and direct reaction potentials.

$E_{\rm c.m.}$ (MeV)	a_F (fm)	$r_{\rm DR}$(fm)	χ^2/N
31.05	0.570	1.61	0.21
32	0.513	1.63	0.65
32.94	0.560	1.63	0.45
34.82	0.534	1.66	0.56
36.7	0.670	1.67	0.90
38.59	0.670	1.68	0.90

The straight lines in Fig. 1(a) are linear fits to the extracted potentials; these lines are used to integrate the dispersion relation. The curves in Fig. 1(b) correspond to this integration for the real polarization potentials $V_F(E)$ and $V_{\rm DR}(E)$. As can be observed, our calculations show that the dispersion relation is satisfied. Also, it is interesting to point out that the surface real potential $V_{\rm DR}(E)$ becomes repulsive for the whole energy range studied (above the experimental barrier energy $V_B = 31.05$ MeV).

The results of the simultaneous fits of the elastic scattering and complete fusion with the potential strengths of Fig. 1 with diffuseness and radial parameters of Table I are shown in Figs. 2 and 3, respectively. Figure 3 also shows the total

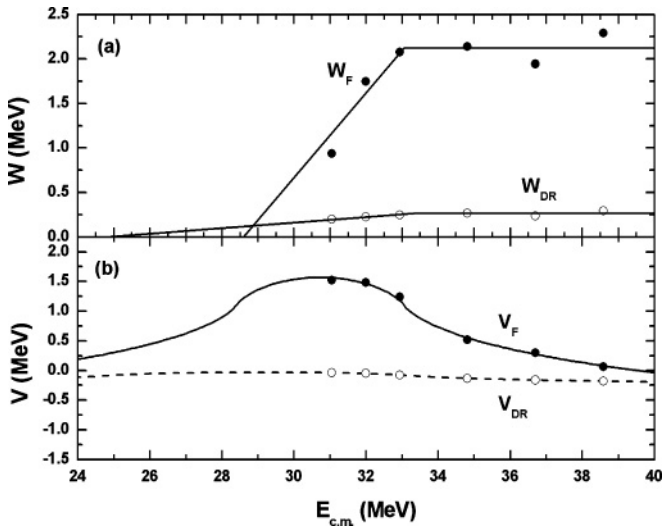

FIG. 1. Potential strengths as derived from the χ^2 analysis for the fusion and direct reaction potentials (dots). The lines in part (a) correspond to linear fits; those in part (b) are the results of the dispersion relation.

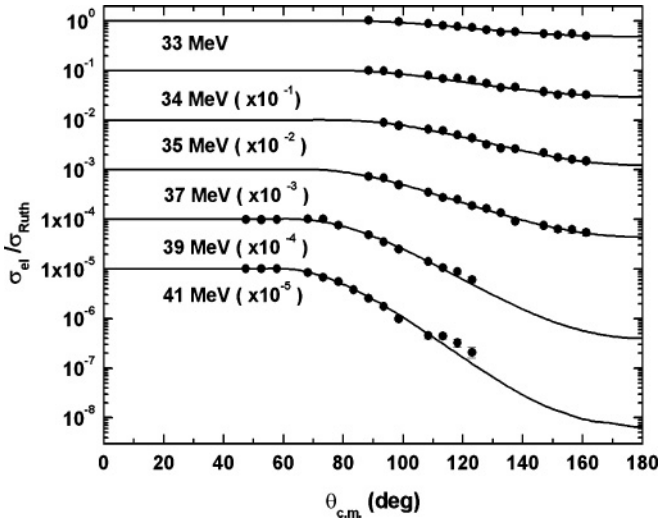

FIG. 2. Results of the ratios of elastic scattering cross sections to Rutherford cross sections. The experimental data are taken from Ref. [18].

reaction cross sections derived from the elastic scattering data and/or calculations by using the potential that fits these data. The calculations were performed by using the FRESCO code [73]. In Fig. 4, the calculations for σ_R-σ_{CF} are given in comparison with the data for $\sigma_{NCBU} + \sigma_{ICF} + \sigma_{inel}$ extracted from Refs. [18,42]. It should be pointed out that σ_R-σ_{CF} corresponds to the calculation of the direct reaction cross section using Eq. (12).

B. The threshold anomaly

One of the most interesting features of this model, that of separating the incident flux absorption into fusion and direct reaction parts, represented by the potentials W_F, V_F and W_{DR}, V_{DR}, respectively, is that it allows us to study their

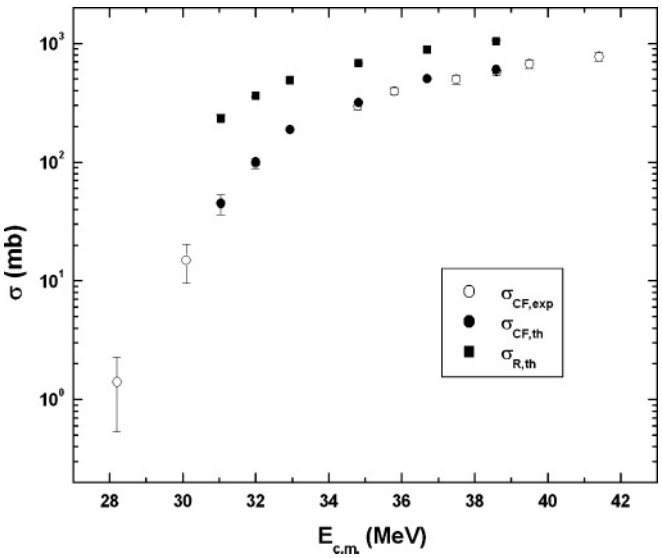

FIG. 3. Calculated complete fusion and total reaction cross sections. The data are those of Ref. [18].

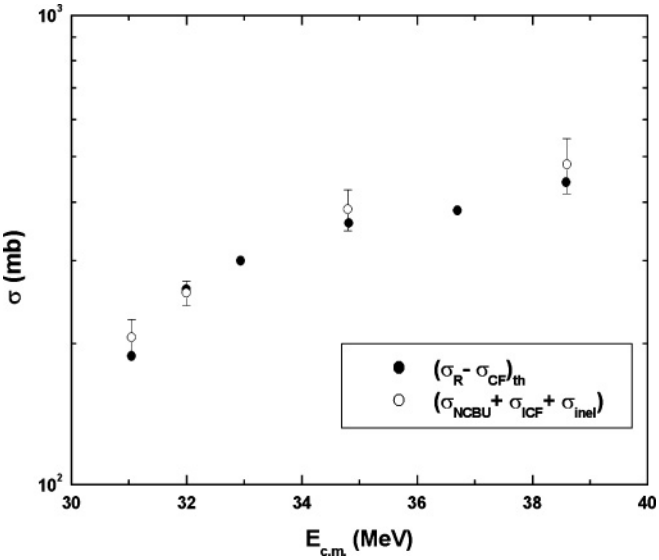

FIG. 4. Results of the direct reaction cross section $\sigma_{DR} = \sigma_R$-σ_{CF}, compared to the corresponding data [18].

energy variation in a separate manner. As can be observed in Figs. 1(a) and 1(b), W_F and V_F show a strong variation around the barrier energy, which is characteristic of the TA usually present in reactions between stable tightly bound nuclei. However, W_{DR} and V_{DR} do not seem to present this strong variation, since they are rather smooth functions of E. However, because the geometric forms of the fusion and direct reaction potentials are different, the potential strengths of Figs. 1(a) and 1(b) cannot by themselves provide enough information on the relative importance of both mechanisms in the region of strong absorption. For this reason, it is convenient to consider their values at the strong absorption radius R_{sa}. At a distance around R_{sa}, different potentials with comparable good fits take approximately the same value. Hence, this value is usually called the sensitivity radius and it is usual procedure to calculate the values of the real and imaginary parts of the optical potential at this distance. Nevertheless, R_{sa} is slightly energy dependent and fluctuates around an average value. For our nuclear system and within the energy range studied, R_{sa} takes values from 11.70 to 11.98 fm, with an average value of $R_{sa} = 11.86$ fm. It is interesting to notice that this value is larger than the radius of the Coulomb barrier, R_B, found to be 10.2 fm. In Figs. 5(a) and 5(b), we present the values of V_F, V_{DR}, W_F, and W_{DR} as functions of the energy at the average strong absorption radius. It can be observed from Fig. 5(b) that in the whole range of energy investigated, $|W_{DR}(R_{sa}, E)|$ is larger than $|W_F(R_{sa}, E)|$, which means that flux absorption is dominated by direct reactions at this distance. Owing to the predominance of $W_{DR}(R_{sa}, E)$ in the total potential $W(R_{sa}, E) = W_F(R_{sa}, E) + W_{DR}(R_{sa}, E)$, one can conclude that the total imaginary potential does not show a sharp decrease as the energy is lowered toward the barrier $V_B = 31.05$ MeV. One can also observe from Fig. 5(a) that the surface real potential $V_{DR}(R_{sa}, E)$, being repulsive, dominates over the fusion counterpart $V_F(R_{sa}, E)$, and the total potential $V(R_{sa}, E) = V_F(R_{sa}, E) + V_{DR}(R_{sa}, E)$ seems to have a very different energy variation from the usual bell

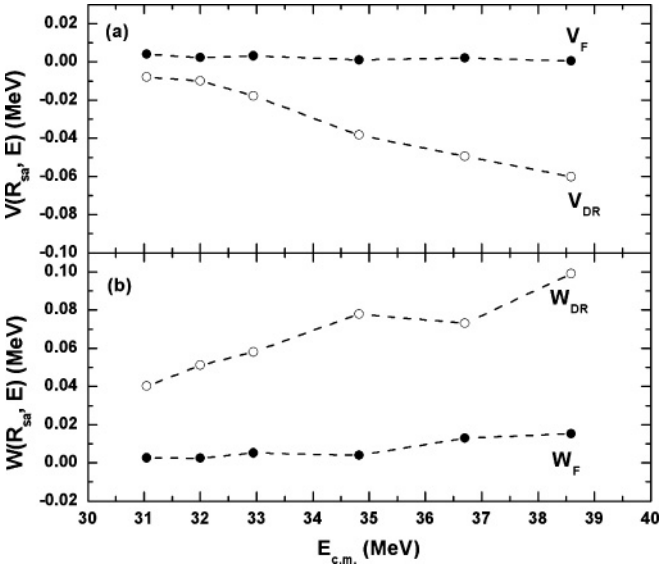

FIG. 5. Real (a) and imaginary (b) fusion and direct reaction polarization potentials at the strong absorption radius R_{sa}. The linear segments are drawn to guide the eye.

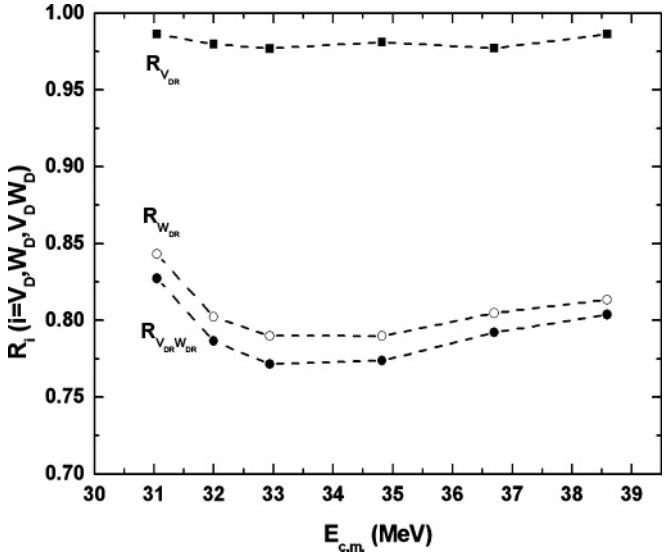

FIG. 6. Ratios R_i of the calculated complete fusion cross sections for the cases $i = V_{DR}$, W_{DR}, and $V_{DR}W_{DR}$ to the the case when $V_{DR} = 0$, $W_{DR} = 0$. The linear segments are drawn to guide the eye.

shape around the barrier, which is a characteristic of the threshold anomaly. From these results, one can conclude that the threshold anomaly is not present for the ^{9}Be + ^{144}Sm system. This finding is in agreement with other previously reported works for different nuclear systems involving weakly bound projectiles and different target masses such as ^{6}Li + ^{208}Pb [6,68], ^{9}Be + ^{64}Zn [17,20], and ^{9}Be + ^{209}Bi [10,68]. We believe that from the present work using two components of the imaginary parts of the optical potential, one can understand more clearly the behavior of the elastic scattering of this weakly bound system.

C. The effect of breakup reactions on fusion

We propose that the effect of breakup reactions on the fusion cross section of weakly bound systems can be studied by "turning on" and "off" the part of the potential that is responsible for direct reactions, that is, V_{DR} and W_{DR}. This can be assumed since, for such systems, breakup is by far the most important contribution to the direct reaction cross section. From Fig. 5 one can conclude that there are two main effects by which V_{DR} and W_{DR} may affect fusion reactions. (i) A repulsive V_{DR} tends to raise the Coulomb barrier and therefore to suppress fusion. (ii) The loss of incident flux into direct reactions, represented by W_{DR}, suppresses fusion. So, one can isolate the separate effect of breakup on fusion from V_{DR} and/or W_{DR} by analyzing the energy dependence of the quantities R_i given by

$$R_i = \sigma_F(i)/\sigma_F(V_{DR} = W_{DR} = 0); \qquad i = V_{DR}, W_{DR}, V_{DR}W_{DR}. \tag{13}$$

In Eq. (13), $\sigma_F(i)$ means fusion cross section when the potential i is considered. The situation when both $V_{DR}W_{DR}$ are used, that is,$\sigma_F(V_{DR}W_{DR})$, corresponds to our final calculation for the CF cross sections. Figure 6 shows the results for R_i for the energy range studied. As expected, a repulsive real potential V_{DR} suppresses fusion, so that $R_{V_{DR}} < 1$. Also, W_{DR}, which is connected to the loss of flux mainly into the breakup channel, also suppresses fusion. When both potentials V_{DR} and W_{DR} are simultaneously applied, we obtain a net fusion suppression. This result is in agreement with some other works where experimental complete fusion cross sections are compared with coupled channel calculations that use potentials deduced from experimental barrier distributions [71,72,74] or reliable double-folding potentials [18,42,75–78] that do not take into account the breakup channel.

IV. SUMMARY AND CONCLUSIONS

In summary, we have carried out a simultaneous χ^2 analysis of elastic scattering and complete fusion cross sections for the system ^{9}Be + ^{144}Sm at near-fusion-barrier energies. In the model, the optical polarization potential has been split into fusion and direct reaction parts. The results of the χ^2 fitting show that the extracted potentials satisfy the dispersion relation. It has been shown that the fusion potential $W_F(E)$ exhibits the threshold anomaly as it usually occurs in reactions with tightly bound projectiles. However, this is not the case for the surface potential $W_{DR}(E)$, which becomes a smooth function of E. Energy-dependent forms for V_F, V_{DR}, W_F, and W_{DR} at the strong absorption radius show that the direct reaction potentials are much more important than the fusion potential. The total imaginary potential $W(R_{sa}, E)$, being the sum of the fusion W_F and direct reaction W_{DR} potentials, is a smooth function of E. However, the real potential $V_{DR}(R_{sa}, E)$ is repulsive around the barrier. All of these facts indicate that the threshold anomaly does not show up from the present analysis. This finding has been found in other calculations that involve the projectile ^{9}Be. However, we believe that the

method used in this work is more illustrative for this kind of analysis than the ones that do not split the imaginary potential. The effect of breakup reactions on fusion cross sections has also been studied by considering the effect on fusion from the potentials responsible for direct reactions (i.e., $V_{\rm DR}$ and $W_{\rm DR}$). By separately considering these potentials, regions of fusion enhancement or suppression could, in principle, be distinguished. However, it has been determined that there is a net effect of suppression of complete fusion cross sections for energies above the Coulomb barrier energy.

ACKNOWLEDGMENTS

P.R.S.G. and J.L. acknowledge the financial support from CNPq and FAPERJ.

[1] M. A. Nagarajan, C. C. Mahaux, and G. R. Satchler, Phys. Rev. Lett. **54**, 1136 (1985).
[2] C. Mahaux, H. Ngô, and G. R. Satchler, Nucl. Phys. **A449**, 354 (1986).
[3] M. S. Hussein, P. R. S. Gomes, J. Lubian, and L. C. Chamon, Phys. Rev. C **73**, 044610 (2006).
[4] M. S. Hussein, P. R. S. Gomes, J. Lubian, and L. C. Chamon, Phys. Rev. C **76**, 019902(E) (2007).
[5] P. R. S. Gomes *et al*., J. Phys. G **31**, S1669 (2005).
[6] N. Keeley *et al*., Nucl. Phys. **A571**, 326 (1994).
[7] N. Keeley and K. Rusek, Phys. Lett. **B427**, 1 (1998).
[8] R. J. Woolliscroft *et al*., Phys. Rev. C **68**, 014611 (2003).
[9] R. J. Woolliscroft *et al*., Phys. Rev. C **69**, 044612 (2004).
[10] C. Signorini *et al*., Phys. Rev. C **61**, 061603(R) (2000).
[11] C. Signorini *et al*., Eur. Phys. J. A **2**, 227 (1998).
[12] C. Signorini, Eur. Phys. J. A **13**, 129 (2002).
[13] S. B. Moraes *et al*., Phys. Rev. C **61**, 064608 (2000).
[14] I. Padron *et al*., Phys. Rev. C **66**, 044608 (2002).
[15] J. Lubian *et al*., Phys. Rev. C **64**, 027601 (2001).
[16] P. R. S. Gomes *et al*., Phys. Lett. **B601**, 20 (2004).
[17] P. R. S. Gomes *et al*., Phys. Rev. C **71**, 034608 (2005).
[18] P. R. S. Gomes *et al*., Phys. Rev. C **73**, 064606 (2006).
[19] P. R. S. Gomes *et al*., Phys. Rev. C **70**, 054605 (2004).
[20] P. R. S. Gomes *et al*., Acta Phys. Hung. New Series - Heavy Ion Phys. **11**, 361 (2000).
[21] J. M. Figueira *et al*., Phys. Rev. C **73**, 054603 (2006).
[22] J. M. Figueira *et al*., Phys. Rev. C **75**, 017602 (2007).
[23] J. O. Fernandez Niello *et al*., Nucl. Phys. **A787**, 484c (2007).
[24] G. V. Marti *et al*., Phys. Rev. C **71**, 027602 (2005).
[25] J. Lubian *et al*., Nucl. Phys. **A791**, 24 (2007).
[26] R. M. Anjos *et al*., Phys. Lett. **B534**, 45 (2002).
[27] A. Pakou *et al*., Phys. Lett. **B556**, 21 (2003).
[28] A. Pakou *et al*., Phys. Rev. C **69**, 054602 (2004).
[29] A. Pakou *et al*., Phys. Rev. Lett. **90**, 202701 (2003).
[30] A. Pakou *et al*., Phys. Rev. C **71**, 064602 (2005).
[31] A. M. M. Maciel *et al*., Phys. Rev. C **59**, 2103 (1999).
[32] E. F. Aguilera *et al*., Phys. Rev. Lett. **84**, 5058 (2000).
[33] E. F. Aguilera *et al*., Phys. Rev. C **63**, 061603(R) (2001).
[34] E. A. Benjamim *et al*., Phys. Lett. **B647**, 30 (2007).
[35] R. Lichtenthäler *et al*., Eur. Phys. J. Spec. Top. **150**, 27 (2007).
[36] A. R. Garcia *et al*., Phys. Rev. C **76**, 067603 (2007).
[37] A. M. Sánchez-Bénitez *et al*., Nucl. Phys. **A803**, 30 (2008).
[38] A. Gomez Camacho, P. R. S. Gomes, J. Lubian, E. F. Aguilera, and I. Padron, Phys. Rev. C **76**, 044609 (2007).
[39] A. Bonaccorso and F. Carstoiu, Nucl. Phys. **A706**, 322 (2002).
[40] A. A. Ibraheem and A. Bonaccorso, Nucl. Phys. **A748**, 414 (2005).
[41] A. Bonaccorso and D. M. Brink, Phys. Rev. C **43**, 299 (1991).
[42] P. R. S. Gomes *et al*., Phys. Lett. **B634**, 356 (2006).
[43] A. Gomez-Camacho, E. Aguilera, P. R. S. Gomes, J. Lubian, and I. Padron, Nucl. Phys. **A787**, 275c (2007).
[44] R. A. Broglia and A. Winther, *Heavy Ion Reactions, Elastic and Inelastic Reactions,* Vol. I (Benjamin-Cummings, Reading, MA, 1981).
[45] R. A. Broglia and A. Winther, *Frontiers in Physics Lecture Notes Series: Heavy Ion Reactions,* Vol. 84 (Addison-Wesley, Reading. MA, 1991).
[46] D. M. Brink, *Semiclassical Methods for Nucleus-Nucleus Scattering* (Cambridge University Press, Cambridge, UK).
[47] G. Pollarolo, L. S. Ferreira, R. J. Liotta, and E. Maglione, Phys. Rev. C **59**, 1534 (1999).
[48] G. Pollarolo and A. Winther, Phys. Rev. C **62**, 054611 (2000).
[49] C. H. Dasso and G. Pollarolo, Phys. Rev. C **68**, 054604 (2003).
[50] G. R. Satchler, Phys. Rep. **199**, 147 (1991).
[51] G. R. Satchler and W. G. Love, Phys. Rep. **55**, 183 (1979).
[52] M. A. Nagarajan and G. R. Satchler, Phys. Lett. **B173**, 29 (1986).
[53] G. R. Satchler, M. A. Nagarajan, J. S. Lilley, and I. J. Thompson, Ann. Phys. (NY) **178**, 110 (1987).
[54] I. J. Thompson, M. A. Nagarajan, J. S. Lilley, and B. R. Fulton, Phys. Lett. **B157**, 250 (1985).
[55] T. Udagawa and T. Tamura, Phys. Rev. C **29**, 1922 (1984).
[56] T. Udagawa, B. T. Kim, and T. Tamura, Phys. Rev. C **32**, 124 (1985).
[57] S. W. Hong, T. Udagawa, and T. Tamura, Nucl. Phys. **A491**, 492 (1989).
[58] B. T. Kim, M. Naito, and T. Udagawa, Phys. Lett. **B237**, 19 (1990).
[59] B. T. Kim, W. Y. So, S. W. Hong, and T. Udagawa, Phys. Rev. C **65**, 044616 (2002).
[60] C. Tenreiro *et al*., Phys. Rev. C **49**, 1218 (1994).
[61] T. Udagawa, T. Tamura, and B. T. Kim, Phys. Rev. C **39**, 1840 (1989).
[62] G. R. Satchler, *Direct Nuclear Reactions* (Clarendon Press, Oxford, 1983).
[63] A. Gómez Camacho, E. M Quiroz, and T. Udagawa, Nucl. Phys. **A635**, 346 (1998).
[64] A. Gómez Camacho and T. Udagawa, Rev. Mex. Fís. **44**, 85 (1998).
[65] A. Gómez-Camacho, E. F. Aguilera, and A. M. Moro, Nucl. Phys. **A762**, 216 (2005).
[66] T. Udagawa, S.-W. Hong, and T. Tamura, Phys. Rev. C **32**, 435 (1985).
[67] T. Udagawa, M. Naito, and B. T. Kim, Phys. Rev. C **45**, 876 (1992).
[68] W. Y. So, S. W. Hong, B. T. Kim, and T. Udagawa, Phys. Rev. C **69**, 064606 (2004).
[69] W. Y. So, S. W. Hong, B. T. Kim, and T. Udagawa, Phys. Rev. C **72**, 064602 (2005).
[70] L. F. Canto, P. R. S. Gomes, R. Donangelo, and M. S. Hussein, Phys. Rep. **424**, 1 (2006).

[71] M. Dasgupta *et al*., Phys. Rev. Lett. **82**, 1395 (1999).
[72] M. Dasgupta *et al*., Phys. Rev. C **70**, 024606 (2004).
[73] I. J. Thompson, Comput. Phys. Rep. **7**, 167 (1988).
[74] M. Dasgupta *et al*., Phys. Rev. C **66**, 041602(R) (2002).
[75] R. Raabe *et al*., Nature **431**, 823 (2004).
[76] E. Crema, L. C. Chamon, and P. R. S. Gomes, Phys. Rev. C **72**, 034610 (2005).
[77] E. Crema, P. R. S. Gomes, and L. C. Chamon, Phys. Rev. C **75**, 037601 (2007).
[78] E. Crema, P. R. S. Gomes, and L. C. Chamon, Nucl. Phys. **A787**, 225c (2007).